ChemComm

Accepted Manuscript

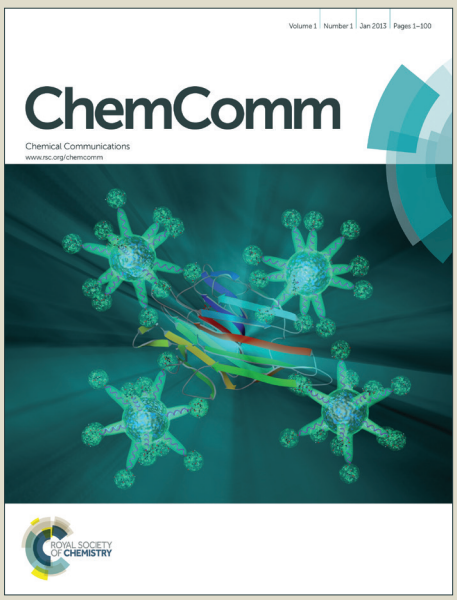

ROYAL SOCIETY OF CHEMISTRY

www.rsc.org/chemcomm

A SERS active bimetallic core-satellite nanostructure for the ultrasensitive detection of Mucin-1

Jingjing Feng, Xiaoling Wu, Wei Ma, Hua Kuang, Liguang Xu, Chuanlai Xu*

Received (in XXX, XXX) Xth XXXXXXXXX 201X, Accepted Xth XXXXXXXXX 201X
First published on the web Xth XXXXXXXXX 201X
DOI: 10.1039/b000000x

In this study, we established gold nanorods (Au NRs) core-silver nanoparticles (Ag NPs) satellite assemblies as an ultrasensitive aptamer-based SERS sensor for the detection of Mucin-1, a specific breast cancer marker protein. The limit of detection (LOD) was 4.3 aM and the wide linear range was 0.005-1 fM.

Cancer is a fatal disease with a high mortality rate, and the global burden of cancer continues to increase[1]. Breast cancer is the most frequently diagnosed cancer and the leading cause of cancer death among females worldwide[2]. Despite diagnostic improvements during the last few decades, the detection of breast cancer in the early stages is still a huge challenge[3-5]. Sensitive monitoring of tumor biomarkers in the blood or other body fluids is an effective diagnostic method for the early detection of malignancies[6]. Mucin-1, which is abnormally expressed in diseased tissues compared with normal tissues, is the most common tumor marker used to diagnose breast tumors[7, 8]. Therefore, enhancing the detection level of Mucin-1 using an ultrasensitive and highly selective analytical assay plays an important role in the early diagnosis of breast cancer.

To date, only a few studies have investigated the identification and quantification of Mucin-1, and the techniques used have included an antibody-mediated Si nanowire field-effect electrical sensor[6], a graphene oxide-based fluorescent aptasensor[7], and an aptamer-antibody hybrid sandwich ELISA[9]. These studies provided a novel concept for the diagnosis of breast cancer in the early stages. However, the antibody was expensive and the enzyme labeling procedure was complicated, the graphene oxide-based modification steps were tedious and the sensing sensitivity was limited. Thus, a rapid detection technique with high selectivity and sensitivity, for early diagnosis with the potential for further improvement is needed.

Surface enhanced Raman scattering (SERS), is a promising ultra-sensitive technique for chemical and biological molecular species, and has received significant attention[10-13]. The merits of SERS include fast detection time, highly sensitive detection over a wide range of excitation wavelengths, and excellent reproducibility with a relative standard deviation. Importantly, metallic nanostructures are frequently used as SERS substrates and have been shown to be associated with enhanced intensity of characteristic spectral signals[11, 14-18]. This enhanced intensity is largely attributed to high local electromagnetic field intensities generated in the vicinity of the metal nanoparticles. In particular, it has been demonstrated that strongly coupled plasmonic assemblies have intense electromagnetic hot-spots and can yield extraordinary enhancement factors for SERS[14, 19-24]. For instance, Gandra and his co-workers[25] found that the core-satellite structures assembled by gold nanoparticles could lead to a remarkable enhancement of Raman scattering by the synergistic combination of many in-built electromagnetic hot-spots among assemblies. Interestingly, the number of nanoparticles in the assemblies had a great influence on the intensity of SERS which could be significantly improved the sensitivity of detection.

In this study, a novel assembled structure with gold nanorod (Au NR) as a core and multiple silver nanoparticles (Ag NPs) as satellites were constructed. Ag NPs were demonstrated as perfect candidates for SERS probes with higher enhancement than gold nanoparticles[26]. Importantly, due to rod-like gold nanoparticles' intense and aspect ratio-dependent longitudinal surface plasmon resonance, Au NRs with greater local field effect show a huge enhancement of Raman signals[27]. Coupled with many intense electromagnetic hot-spots were developed, the Au NRs core-Ag NPs satellites assemblies could be ideal SERS substrates with expressively improved of the intensity of SERS and sensitivity of detection.

We established the core-satellite structures using DNA as the linker. The aptamer for the designated disease biomarker Mucin-1 and partial complementary sequences were coupled to the Ag NPs and Au NRs, respectively. The functionalized nanostructures were then mixed with the Au NRs core-Ag NPs satellite assemblies following DNA hybridization in the absence of the target Mucin-1, as illustrated in Scheme 1. Subsequently, in the presence of Mucin-1, the high specific biorecognition of aptamer and Mucin-1 caused the release of the core-satellite assemblies. As the SERS intensity of core-satellites superstructures was in proportion to the number of satellite Ag NPs around the core AuNRs, it was significantly decreased with increased concentration of Mucin-1. Furthermore, to evaluate the sensitivity of this biosensing system, SERS spectra of core-satellite assemblies composed in the presence of various Mucin-1 concentrations were measured and were quantified in a wide linear range, using the characteristic SERS peak of the Raman reporter molecule (4-aminothiophenol, 4-ATP) at 1142 cm^{-1}.

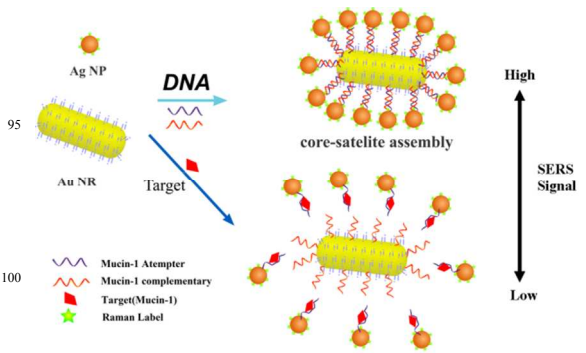

Scheme 1. Scheme of SERS aptasensor for the detection of Mucin-1 based on Au NRs-Ag NPs core-satellite assemblies.

Ag NPs with a diameter of 10±1.3 nm were prepared using a previously published method with modifications[28,29], and the slightly improved seed-mediated growth method was used for the controllable synthesis of Au NRs[11]. The synthesized Ag NPs and Au NRs were then characterized using transmission electron microscopy (TEM) and ultraviolet-visible (UV-Vis) absorption spectra, as shown in Figs. S1 and S2. To obtain the core-satellite assemblies, thiol-modified Mucin-1 aptamers with the sequence of 5′-SH-AAAAAGCAGTTGATCCTTTG GATACCCTGGT-3′ were added to Ag NPs in a mole ratio of 5:1, and the Au NRs were functionalized simultaneously with the Mucin-1 complementary sequence of 5′-SH-AAAAAATCCAAAGGATG TTCTG-3′ at a coupling ratio of 500 to 1. After the mixtures were allowed to react at room temperature for 12 h with gentle shaking, respectively, Ag NPs-aptamers were mixed with Au NRs-complementary along with gentle shaking for several minutes. Following a prolonged hybridization time, the representative TEM images of the satellites are shown in Fig. S3 with the number of Ag NPs gradually increasing around the core Au NRs, and the assembly reaction was complete within 12 h. The intensity of SERS enhancement was characterized by the representative SERS spectra of the reacted satellite assembly solutions with 10 μM 4-ATP for different hybridization times (0, 6 h, 12 h), as shown in Fig. S4. The Raman spectrometer with an air-cooled He-Ne laser was selected 633 nm excitation with a laser power of ~8 mW and the Raman spectra were acquired from the substrates for an accumulation time of 10 s.

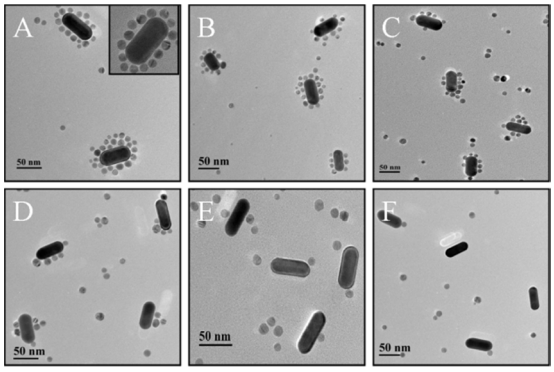

Figure 1. TEM images of Au NRs-Ag NPs core-satellite assemblies with different concentrations of Mucin-1. (A) 0 fM, (B) 0.005 fM, (C) 0.01 fM, (D) 0.05 fM, (E) 0.1 fM, and (F) 1 fM.

For Mucin-1 detection, various concentrations (0, 0.005, 0.01, 0.05, 0.1, and 1 fM) of Mucin-1 were respectively added to the reacted satellite assembly solutions, and then analyzed by TEM, UV-Vis and Raman spectra. From the TEM images of core-satellite assemblies shown in Figure 1, it was observed that as the concentration of Mucin-1 gradually increased, the average number of Ag NPs around the Au NRs decreased. The highest assembly efficiency was obtained when no Mucin-1 was added, and there were only a few satellite Ag NPs surrounding the core Au NRs when the Mucin-1 concentration added was 1 fM. UV-Vis spectra at different concentrations of Mucin-1 are shown in Fig. S5, where the UV-Vis signals showed no obvious change. Moreover, the characteristic 4-ATP SERS peak at 1142 cm^{-1} was used in the quantitative analysis of Mucin-1. Figure 2A shows the SERS spectra at different concentrations of Mucin-1. The standard curve was plotted for 1142 cm^{-1} against the logarithm of the Mucin-1 concentration over the range of 0.005 to 1 fM, and a correlation coefficient (R^2) of 0.9969 and an LOD of 4.3 aM were obtained by multiplying the standard deviation of the blanks by three, as shown in Figure 2B.

To evaluate the selectivity of this method, six other cancer marker proteins, including AFP (Alpha-feto Protein), PSA (Prostate Specific Antigen), HAS (human serum albumin), BSA (Bovine Serum Albumin), Thrombin, and VEGF (Vascular Endothelial Growth Factor) all at the same concentration of 50 fM, were tested under the same conditions (Figure 3). Simultaneously, 0.5 fM of Mucin-1 and the control without any target and interferences were added. Despite the concentration being 100-fold higher than Mucin-1, the SERS intensity of these proteins showed no obvious reduction compared with the control, while Mucin-1 was markedly reduced, which confirmed the high specificity of the established Mucin-1 detection sensor.

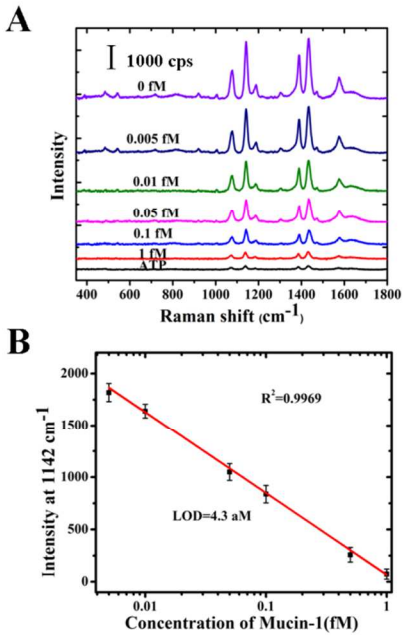

Figure 2. Mucin-1 detection based on SERS with Au NRs-Ag NPs core-satellite assemblies (A) SERS spectra of Mucin-1 detection. (B) Standard curve for Mucin-1 detection with corresponding peak intensities at 1142 cm^{-1}.

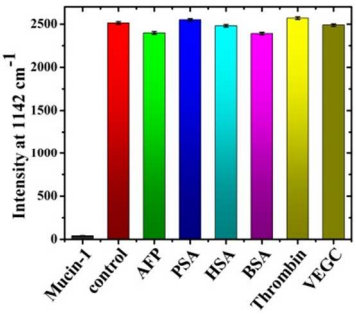

Figure 3. Selectivity of the SERS active platform toward Mucin-1 against other cancer marker proteins. The Raman values of the proposed sensor after the hybridization with different targets: Mucin-1 (0.5 fM), AFP (50 fM), PSA (50 fM), HAS (50 fM), BSA (50 fM), Thrombin (50 fM), VEGC (50 fM).

The reliability of the developed approach was examined by analyzing Mucin-1 in serum samples, which were obtained from the Second Hospital in Wuxi, P.R.C, and the Mucin-1 concentrations were determined by a standard clinical diagnostic assay (ADVIA Centaur, Siemens). The samples were diluted 1000 times and the results are shown in Table 1. The detected concentrations were almost consistent, indicating that this assay is a feasible and promising method for clinical applications.

M), VEGC (50 fM). Control was no any targets spiked in.

Table 1. Practical analysis of Mucin-1 in human blood serum

Serum samples[a]	Original Concentration[b] (μM)	Diluted Concentration[c] (fM)	Detected Concentration[d] (fM)
1	0.89	0.89	0.91±0.02
2	0.56	0.56	0.55±0.02
3	0.13	0.13	0.11±0.03

[a] Serum sample were human sera sampling from three donors at the Second People's Hospital of Wuxi, P.R.C.
[b] Original concentrations of Mucin-1 in serum samples were determined by the standard clinical diagnostic assay (ADVIA Centaur, Siemens).
[c] Original serum samples were serially diluted and then stood for at least 2 h before the determination.
[d] SD was calculated based on four parallel experiments for each sample.

In summary, a SERS sensor with significant specificity and practicability for the detection of Mucin-1 was developed, based on the first report of Au NRs-Ag NPs core-satellite nanostructures. The limit of detection for Mucin-1 was 4.3 aM, the lowest value reported so far. Moreover, this method may be used as a promising technology for the early monitoring of breast cancer in the future.

Acknowledgements

This work is financially supported by the National Natural Science Foundation of China (21371081, 21301073).

Notes and references

State Key Lab of Food Science and Technology, School of Food Science and Technology, Jiangnan University, Wuxi, JiangSu, 214122, P. R. China. E-mail: xcl@jiangnan.edu.cn

† Electronic Supplementary Information (ESI) available: [details of any supplementary information available should be included here]. See DOI: 10.1039/b000000x/

1. L. A. Torre, F. Bray, R. L. Siegel, J. Ferlay, J. Lortet-Tieulent and A. Jemal, *CA: a cancer journal for clinicians*, 2015, **65**, 87-108.
2. M. Debald, W. Kuhn and O. Golubnitschaja, *EPMA Journal*, 2014, **5**, A41.
3. A. Goldhirsch, E. P. Winer, A. S. Coates, R. D. Gelber, M. Piccart-Gebhart, B. Thurlimann, H. J. Senn and m. Panel, *Annals of oncology : official journal of the European Society for Medical Oncology / ESMO*, 2013, **24**, 2206-2223.
4. D. Madhavan, M. Wallwiener, K. Bents, M. Zucknick, J. Nees, S. Schott, K. Cuk, S. Riethdorf, A. Trumpp, K. Pantel, C. Sohn, A. Schneeweiss, H. Surowy and B. Burwinkel, *Breast cancer research and treatment*, 2014, **146**, 163-174.
5. R. Weissleder and M. J. Pittet, *Nature*, 2008, **452**, 580-589.
6. G. Zheng, F. Patolsky, Y. Cui, W. U. Wang and C. M. Lieber, *Nature biotechnology*, 2005, **23**, 1294-1301.
7. Y. He, Y. Lin, H. Tang and D. Pang, *Nanoscale*, 2012, **4**, 2054-2059.
8. X. Zhu, J. Yang, M. Liu, Y. Wu, Z. Shen and G. Li, *Analytica chimica acta*, 2013, **764**, 59-63.
9. C. S. M. Ferreira, K. Papamichael, G. Guilbault, T. Schwarzacher, J. Gariepy and S. Missailidis, *Analytical and Bioanalytical Chemistry*, 2007, **390**, 1039-1050.
10. P. Guo, D. Sikdar, X. Huang, K. J. Si, W. Xiong, S. Gong, L. W. Yap, M. Premaratne and W. Cheng, *Nanoscale*, 2015, **7**, 2862-2868.
11. W. Ma, H. Kuang, L. Xu, L. Ding, C. Xu, L. Wang and N. A. Kotov, *Nature communications*, 2013, **4**, 2689.
12. L. Xu, C. Hao, H. Yin, L. Liu, W. Ma, L. Wang, H. Kuang and C. Xu, *The Journal of Physical Chemistry Letters*, 2013, **4**, 2379-2384.
13. S. Li, L. Xu, W. Ma, H. Kuang, L. Wang and C. Xu, *Small*, 2015, DOI: 10.1002/smll.201403356.
14. P. P. Patra, R. Chikkaraddy, R. P. Tripathi, A. Dasgupta and G. V. Kumar, *Nature communications*, 2014, **5**, 4357.
15. V. V. Thacker, L. O. Herrmann, D. O. Sigle, T. Zhang, T. Liedl, J. J. Baumberg and U. F. Keyser, *Nature communications*, 2014, **5**, 3448.
16. Y. Zhu, L. Xu, W. Ma, Z. Xu, H. Kuang, L. Wang and C. Xu, *Chemical communications*, 2012, **48**, 11889-11891.
17. W. Ma, M. Sun, L. Xu, L. Wang, H. Kuang and C. Xu, *Chemical communications*, 2013, **49**, 4989-4991.
18. L. Xu, H. Kuang, C. Xu, W. Ma, L. Wang and N. A. Kotov, *Journal of the American Chemical Society*, 2012, **134**, 1699-1709.
19. W. Ma, H. Kuang, L. Wang, L. Xu, W. S. Chang, H. Zhang, M. Sun, Y. Zhu, Y. Zhao, L. Liu, C. Xu, S. Link and N. A. Kotov, *Scientific reports*, 2013, **3**, 1934.
20. W. Ma, H. Yin, L. Xu, X. Wu, H. Kuang, L. Wang and C. Xu, *Chemical communications*, 2014, **50**, 9737-9740.
21. X. Zhang, Y. Zheng, X. Liu, W. Lu, J. Dai, D. Y. Lei and D. R. MacFarlane, *Advanced materials*, 2015, **27**, 1090-1096.
22. X. Li, W. C. H. Choy, X. Ren, D. Zhang and H. Lu, *Advanced Functional Materials*, 2014, **24**, 3114-3122.
23. Y. W. Katrin Kneipp, Harald Kneipp, Lev T. Perelman, Irving Itzkan, and a. M. S. F. Ramachandra R. Dasari, 1997.
24. L. Tang, S. Li, F. Han, L. Liu, L. Xu, W. Ma, H. Kuang, A. Li, L. Wang and C. Xu, *Biosensors & bioelectronics*, 2015, **71**, 7-12.
25. N. Gandra, A. Abbas, L. Tian and S. Singamaneni, *Nano letters*, 2012, **12**, 2645-2651.
26. J. Zhao, A. O. Pinchuk, J. M. McMahon, S. Li, L. K. Ausman, A. L. Atkinson and G. C. Schatz, *Acc. Chem. Res.*, 2008, **41**,1710-1720.
27. M. D. Doherty, A. Murphy, R. J. Pollard and P. Dawson, *Physical Review X*, 2013, **3**, 1-11.
28. X. Wu, L. Xu, L. Liu, W. Ma, H. Yin, H. Kuang, L. Wang, C. Xu and N. A. Kotov, *Journal of the American Chemical Society*, 2013, **135**, 18629-18636.
29. W. Yan, L. Xu, C. Xu, W. Ma, H. Kuang, L. Wang and N. A. Kotov, *Journal of the American Chemical Society*, 2012, **134**, 15114-15121.